CONCENTRATION DEPENDENCE OF IN VITRO BIOTRANSFORMATION RATES OF HYDROPHOBIC ORGANIC SUNSCREEN AGENTS IN RAINBOW TROUT S9: IMPLICATIONS FOR BIOACCUMULATION ASSESSMENT.

Leslie J. Saunders[†], **Simon Fontanay**[‡], **John W. Nichols**[#], and **Frank A.P.C. Gobas**[§]

[†]Department of Biological Sciences, Simon Fraser University, Burnaby, British Columbia, Canada

[‡]Department of Biological Engineering, Polytech Clermont-Ferrand, France

[#]United States Environmental Protection Agency, Duluth, Minnesota, USA

[§]School of Resource and Environmental Management, Simon Fraser University, Burnaby, British Columbia, Canada

Abstract

In-vitro biotransformation studies were performed to support the bioaccumulation assessment of three hydrophobic organic ultraviolet filters (UVFs), 4-methylbenzylidene camphor (4-MBC), 2-ethylhexyl-4-methoxycinnamate (EHMC), and octocrylene (OCT). *In-vitro* depletion rate constants (k_{dep}) were determined for each UVF in rainbow trout liver S9 fractions. Incubations performed with and without added cofactors showed complete (4-MBC) or partial (EHMC and OCT) dependence of k_{dep} on phase I cofactors (NADPH), suggesting that hydrolysis of EHMC and OCT by cofactor-independent enzymes (e.g. carboxylesterases) is an important metabolic route. The concentration dependence of k_{dep} was evaluated to estimate Michaelis-Menten parameters (K_m and V_{max}) for each UVF. Measured k_{dep} values were then extrapolated to apparent whole-body biotransformation rate constants using an *in-vitro* to *in-vivo* (IVIVE) extrapolation model. Bioconcentration factors (BCF) calculated from k_{dep} measured at concentrations well below K_m were closer to empirical BCFs than those extrapolated from k_{dep} measured at higher test concentrations. Modeled BCFs were also sensitive to *in vitro* binding assumptions employed in the IVIVE model, highlighting the need for further characterization of chemical binding effects on hepatic clearance. This study suggests that BCFs of the tested UVFs are expected to be less than 2000 L kg^{-1}, but consideration of appropriate *in-vitro* test concentrations and binding correction factors are important when using IVIVE methods to refine modeled BCFs.

Keywords

bioaccumulation; biotransformation; in vitro in vivo extrapolation; ultraviolet filters; sunscreens

Corresponding author: Frank A.P.C. Gobas School of Resource and Environmental Management, Simon Fraser University, Burnaby, British Columbia, Canada, T: (1) 778.782.5928, F: (1) 778.782.4968, gobas@sfu.ca.

INTRODUCTION

The potential for bioaccumulation in fish and other aquatic species is a critical component in the assessment of commercial chemicals for their risk to the environment and human health. International and national regulations specify criteria for categorizing bioaccumulation behavior based on a chemical's measured bioconcentration factor (BCF), bioaccumulation factor (BAF), and/or octanol-water partition coefficient (K_{OW}) (Gobas et al. 2009). For most chemicals, BCF or BAF data are unavailable, so computational models are often used to estimate a BCF for fish based on a chemical's measured or estimated K_{OW} (Arnot & Gobas 2006). However, if a chemical is biotransformed, a BCF calculated based solely on K_{OW} may overestimate the true extent of accumulation, thereby mischaracterizing that chemical's bioaccumulation potential (Weisbrod et al. 2009; Nichols et al. 2009). This makes biotransformation in fish a key parameter in the bioaccumulation assessment of commercial chemicals.

Biotransformation rates in fish can be measured in controlled *in vivo* experiments (Sijm& Opperhuizen 1989; Sijm et al. 1990; Arnot et al. 2008; Lo et al. 2015b; Lo et al. 2016) but these approaches are costly and labor-intensive, involving efforts similar to those in BCF tests. In addition, such experiments require a large numbers of animals, which is inconsistent with the replacement, reduction, and refinement of animal use promoted under REACH (Laue et al. 2014). Alternatives to animal testing are needed to provide screening-level information that may be used to refine modeled bioaccumulation calculations (Fay et al. 2016). One approach is to use quantitative structure-activity relationship (QSAR) models to estimate biotransformation rates (Arnot et al. 2009). While these models are useful, they are limited by access to empirical data (typically measured BCFs) for development and testing. Another alternative to *in vivo* testing is *in vitro* to *in vivo* extrapolation (IVIVE), whereby chemical biotransformation is measured using an *in vitro* system derived from liver tissue (hepatocytes or subcellular liver preparations) (Han et al. 2007; Cowan-Ellsberry et al. 2008; Han et al. 2009; Mingoia et al. 2010; Connors et al. 2013; Lee et al. 2014; Laue et al. 2014; Lo et al. 2015a; Nichols et al. 2017). This information is then scaled to the intact animal to estimate a whole-body biotransformation rate constant (Han et al. 2007; Cowan-Ellsberry et al. 2008; Han et al. 2009; Laue et al. 2014; Trowell et al. 2018). Results to date show that BCFs calculated by incorporating measured *in vitro* biotransformation rates into established BCF models are much closer to measured values than are BCFs generated under the assumption of no metabolism (Han et al. 2007; Cowan-Ellsberry et al. 2008; Han et al. 2009; Laue et al. 2014). Nevertheless, there is a consistent tendency for these methods to overestimate BCFs relative to empirical BCF values (Han et al. 2009; Laue et al. 2014). This suggests that *in vivo* rates of biotransformation are systematically underestimated by IVIVE methods.

The IVIVE approach assumes that chemical biotransformation occurs predominantly in the liver; extrahepatic biotransformation is generally ignored, as are other potential elimination pathways such as secretion of parent chemical to bile and urine. The IVIVE approach also ignores the possibility that enzyme induction occurs during standardized *in vivo* exposures. With respect to the extrapolation procedure itself, it is assumed that the chemical concentration *in vivo* at the site of biotransformation is well below saturating levels.

Application of the method requires, therefore, that *in vitro* measurements be made under non-saturating (i.e. first-order) conditions. Recent work with trout liver S9 fractions has shown, however, that substrate concentrations commonly used in earlier studies (typically ≥ 1 μM) may saturate biotransformation enzymes (Lo et al. 2015a; Nichols et al. 2017). Another source of uncertainty in IVIVE methods is the effect of chemical binding on calculated hepatic clearance rates. Binding correction factors used to extrapolate *in vitro* data to the intact tissue can have large impacts on estimated biotransformation rates (Nichols et al. 2013b; Laue et al. 2014). Errors with respect to the specification of these factors and/or violations of the assumptions they represent may explain apparent discrepancies between empirical BCFs and BCFs calculated by IVIVE procedures (Nichols et al. 2013a; Laue et al. 2014).

The primary objective of this study was to investigate the *in vitro* biotransformation of three organic ultraviolet filters (UVFs) in rainbow trout: 4-methylbenzylidene camphor (4-MBC), 2-ethylhexyl-4-methoxycinnamate (EHMC), and octocrylene (OCT) (Figure 1). Measureable concentrations of these UVFs have been reported in surface waters, sediments, sewage sludge, and aquatic biota (Nagtegaal et al. 1997; Balmer et al. 2005; Fent et al. 2006; Buser et al. 2006; Zenker et al. 2008; Fent et al. 2010; Bachelot et al. 2012; Gago-Ferrero et al. 2012; Gago-Ferrero et al. 2013; Picot Groz et al. 2014). Concern regarding the bioaccumulation potential of UVFs exists because of their hydrophobicity (log $K_{OW} > 4$). However, measured BCFs (Blüthgen et al. 2014; Li et al. 2016; Sigma-Aldrich 2014; US National Library of Medicine 2006), BAFs (Fent et al. 2010), and biota-sediment accumulation factors (BSAF) (Gago-Ferrero et al. 2015) for the selected UVFs in fish fall well below established bioaccumulation criteria (Table 1), suggesting that fish have the capacity to biotransform these chemicals (Gago-Ferrero et al. 2015). Ester groups present on EHMC and OCT may provide a target for esterases and/or cytochrome P450 (CYP) enzymes. 4-MBC and EHMC are biotransformed by rodents (Völkel et al. 2006; Fennell et al. 2017), but there is limited information available on UVF biotransformation in fish.

In vitro depletion rate constants (k_{dep}) were measured for each UVF using trout liver S9 fractions. The S9 fraction is a "complete" metabolizing system insofar as it contains the full complement of microsomal and cytosolic enzymes. Initial experiments were performed in the presence and absence of phase I and phase II cofactors as a means of exploring potential reaction pathways involved in UVF biotransformation. Additional studies were then conducted to evaluate the *in vitro* concentration dependence of biotransformation, and to estimate Michaelis-Menten parameters (K_m and V_{max}) for each reaction. Finally, a model-based approach was used to evaluate the effects of the initial substrate (UVF) concentration as well as different *in vitro* and *in vivo* binding assumptions on BCFs calculated using IVIVE methods.

MATERIALS AND METHODS

Chemicals

Acetonitrile and hexane were obtained from Caledon Laboratories. Tricaine methanesulfonate (MS 222) was obtained from Syndel. All other chemicals, reagents and

cofactors were obtained from Sigma-Aldrich and were reagent-grade or higher in quality and at purities > 97%.

Liver S9 preparation and characterization

Rainbow trout (*Oncorhynchus mykiss*) were obtained from Miracle Springs Hatchery (Mission, BC, CAN) and the USGS Upper Midwest Environmental Sciences Center (La Crosse, WI, USA). Fish were held in flow-through tanks and were acclimatized for at least 2 weeks before use. Details on study animals and holding conditions are displayed in Table S1.

Fish were euthanized by a 5 min exposure to 0.3 g L^{-1} MS 222 buffered with 0.3 g L^{-1} NaHCO$_3$. Two pools (A and B) of liver S9 fractions were prepared using procedures given by Johanning et al. (Johanning et al. 2012). Homogenization buffers and centrifugation conditions are summarized in the Supplemental Data (Table S1). Aliquots (0.5 mL) of both S9 pools were collected, flash-frozen in liquid nitrogen, and stored at −80 °C until use. The protein concentration of Pool A was determined by the Bradford assay (A rapid and sensitive method for the quantitation of microgram quantities of protein utilizing the principle of protein-dye binding 1976), while that of Pool B was measured by Peterson's modification of the Lowry method (Sigma technical bulletin TP0300; Sigma-Aldrich, St. Louis, MO) using bovine serum albumin (Fraction V) as the standard. Previous investigations show that these two techniques produce very similar estimates of protein content (van den Heuvel et al. 1995). Total lipids were determined in the S9 pools using the Bligh and Dyer method (Bligh & Dyer 1959).

Substrate depletion experiments with pyrene, a well-known substrate for CYP1A, were performed to assess the activity of liver S9 fractions. *In vitro* intrinsic clearance rates averaged 0.33 ± 0.06 mL h^{-1} mg^{-1} S9 protein at 0.78 μM and 0.46 ± 0.1 mL h^{-1} mg^{-1} S9 protein at 0.50 μM for Pools A and B, respectively. Both values are in good agreement with previously determined intrinsic clearance rates for pyrene measured using trout liver S9 fractions (0.36 ± 0.12 mL h^{-1} mg^{-1} S9 protein at 1.0 μM) (Lo et al. 2015a).

Effect of cofactors on biotransformation of UVFs

Substrate depletion experiments with 4-MBC, EHMC, and OCT were performed in 4 different incubation mixtures: (i) Inactivated (heat-treated) S9; (ii) Active S9 incubation with no added cofactors; (iii) Active S9 incubation containing 2.0 mM β-NADPH; (iv) Active S9 incubation containing 2.0 mM β-NADPH, 2.0 mM reduced glutathione (GSH), 0.1 mM 3'phosphoadenosine 5'-phosphosulfate (PAPs), and 5.0 mM uridine 5'-diphosphoglucuronic acid (UDPGA). Incubations performed without added cofactors (test ii) were designed to test for biotransformation by cofactor-independent enzymes such as carboxylesterases, while those performed in the presence of β-NADPH (test iii) and β-NADPH plus phase II cofactors (test iv) were included to evaluate the contribution of CYP and phase II reaction pathways, respectively. Three independent incubations, using a multi-tube approach (Johanning et al. 2012) were conducted. Each experiment included one replicate of each incubation mixture (tests i through iv) to determine a mean *in vitro* depletion rate constant (*n*=3) for each UVF for the tested set of conditions.

Stock solutions of 4-MBC, EHMC, and OCT were prepared in acetonitrile with the goal of achieving a nominal concentration of 0.5 μM in the incubation medium. Experiments were initiated by spiking with 2.4 μL (4-MBC and EHMC) or 5 μL (OCT) of stock solution into an incubation mixture containing S9 protein in 0.2 M pH 7.8 potassium phosphate buffer. Incubations containing 4-MBC and EHMC were performed at 13 °C using 4.3 mg mL^{-1} S9 protein (Pool A) and a final incubation volume of 0.5 mL. Incubations with OCT were performed at 11 °C using 1 mg mL^{-1} S9 protein (Pool B) at a final incubation volume of 1 mL. The volume of acetonitrile in the incubation mixture was always < 0.5% (v/v). Incubations were terminated at regular time intervals (0–90 min) by adding 200 μL ice-cold acetonitrile. Internal standard (d^{12}-chrysene; 5 μL of 0.5 μM) was added to each vial and mixed using a vortex mixer for 10 s. Then, 1.0 mL of n-hexane was added to the vial and the vials were shaken on a vortex mixer for 5 min to extract each UVF and internal standard. Following extraction, the vials were centrifuged at 2000 g for 10 min. The hexane supernatant was transferred to a clean 2 mL amber glass vial (Agilent) for gas chromatography/mass spectrometry (GC/MS) analysis.

First-order depletion rate constants (k_{dep}; min^{-1}) for each UVF were determined as the slope of the relationship between the natural logarithm of measured concentrations and incubation time (t):

$$LnC_t = LnC_0 - k_{dep} \times t \quad (1)$$

where C_0 and C_t are the concentrations of UVF (μM) at time 0 and time t (min).

Mean k_{dep} values derived for each UVF using the 4 different incubation mixtures were evaluated by ANOVA and Tukey's HSD test. If significant UVF depletion was observed in active S9 fractions without added cofactors, subsequent incubations were performed to evaluate the *in vitro* concentration dependence of these reactions with and without cofactors. If the inclusion of the phase II cofactors had no impact on the rate of UVF depletion, then phase II cofactors were omitted from future incubations with added NADPH. All statistical analyses were performed in JMP 10. A *p*-value < 0.05 was considered statistically significant.

Effect of concentration on biotransformation of UVFs

Triplicate incubations were performed for 4-MBC, EHMC, and OCT at 7 or 8 initial concentrations ranging from 0.05 to 12.5 μM. All initial concentrations were well below the estimated solubility of each UVF in the incubation media (Table S2). Independent heat-treated controls were run simultaneously at each concentration. Preliminary experiments were performed to develop sampling protocols for each tested concentration, resulting in sampling schedules that differed somewhat across chemicals and tests.

Depletion rate constants determined for replicate incubations were averaged to calculate a mean k_{dep} for each initial substrate (UVF) concentration (C_0). These mean values were then fitted by weighted nonlinear regression to a re-written form of the Michaelis–Menten equation (Obach & Reed-Hagen 2002; Nath & Atkins 2006):

$$k_{dep} = k_{dep,\,C \to 0} \times \left(1 - \frac{c_0}{C_0 + K_m}\right) \quad (2)$$

where $(k_{dep,C \to 0})$ (min^{-1}) is the *in vitro* depletion rate constant at an infinitesimally low substrate concentration and K_m is the Michaelis-Menten affinity constant (μM) for the reaction. The fitted equation for each UVF was used to obtain estimates of $k_{dep,C \to 0}$ and K_m (JMP 10). The *in vitro* intrinsic clearance rate (CL$_{in\ vitro,\ int}$; mL h^{-1} mg protein^{-1}), which represents enzyme activity under true first-order conditions, was estimated by dividing $k_{dep,C \to 0}$ by the measured protein concentration in the incubation media. The maximum reaction velocity (V_{max}; pmol min^{-1} mg protein^{-1}) was then obtained as the product of CL$_{in\ vitro,\ int}$ and K_m (Nath & Atkins 2006). Importantly, the derived parameters K_m, V_{max}, and CL$_{in\ vitro,\ int}$ reflect the net result of all metabolic pathways operating on the chemical of interest.

GC/MS analysis

Analysis of each UVF and d^{12}-chrysene was performed using an Agilent 6890 gas chromatograph coupled to an Agilent 5973 mass spectrometer and an Agilent 7683 auto sampler (Agilent, Mississauga, ON). The GC was fitted with a cool-on-column capillary inlet and the injection volume was 1 μL. Chemicals were separated on an HP-5MS 5% phenyl methylpolysiloxane-coated column (30 m × 0.25 mm i.d., 0.25 μm film thickness) connected to a fused-silica deactivated guard column (5 m × 0.53 mm i.d.). The oven was held at an initial temperature of 45 °C for 2 min, then increased at 25 °C min^{-1} to 200 °C (0.5 min), followed by an increase at 13 °C min^{-1} to a final temperature of 280 °C (5 min). Helium was used as carrier gas at a constant flow rate of 1.0 mL min^{-1}. Conditions for MS measurements were: electron impact ionization at 70 eV; ion source temperature at 230 °C; selected ions at m/z 254 (4-MBC), 178, 290 (EHMC), 249, 232 (OCT), and 240 (d^{12}-chrysene). Agilent MSD ChemStation software (G1701CA) was used for instrument control and data processing. The calibration curves had strong linearity ($R^2 \geq 0.99$) with constant relative response factors obtained over the range of UVF concentrations.

In vitro to in vivo extrapolation and bioconcentration factors

The k_{dep} values measured at each initial UVF concentration were extrapolated to a set of *in vivo* biotransformation rate constants (k_{MET}; d^{-1}) using an IVIVE model (Nichols et al. 2013b). Estimated k_{MET} values were then used as inputs to a one-compartment bioaccumulation model to derive steady-state BCFs (Arnot & Gobas 2004). The IVIVE model (Nichols et al. 2006; Nichols et al. 2013b) has been outlined previously (Cowan-Ellsberry et al. 2008; Han et al. 2009; Laue et al. 2014). Briefly, k_{dep} was divided by the S9 protein concentration to calculate an apparent *in vitro* intrinsic clearance rate (CL$_{in\ vitro,\ int,\ app}$; mL min^{-1} mg protein^{-1}). Here the term "apparent" is used because many of the calculated values represent rates measured under non first-order conditions. Additional scaling factors were used to extrapolate CL$_{in\ vitro,\ int,\ app}$ to an estimate of *in vivo*

intrinsic clearance ($CL_{in\ vivo,\ int}$; L d^{-1} kg fish^{-1}), which was then employed as an input to a well-stirred liver model (Wilkinson & Shand 1975) to calculate hepatic clearance (CL_H; L d^{-1} kg fish^{-1}):

$$CL_H = \frac{Q_H \times f_U \times CL_{in\ vivo,\ int}}{\left(Q_H + f_U \times CL_{in\ vivo,\ int}\right)} \quad (3)$$

The well-stirred liver model accounts for possible rate limitations imposed by liver blood flow (Q_H; L d^{-1} kg fish^{-1}) on the hepatic clearance rate. This model also includes a parameter, f_U, that corrects for potential binding effects on clearance. The value of f_U is calculated as the ratio of the unbound (or free) chemical fractions in blood plasma (ϕ_P; unitless) and the S9 incubation medium (ϕ_{S9}; unitless):

$$f_U = \frac{\phi_P}{\phi_{S9}} \quad (4)$$

The ϕ_P was calculated as:

$$\phi_P = v_{WBL}/P_{BW} \quad (5)$$

where v_{WBL} is the fractional water content of blood (0.84) and P_{BW} is the equilibrium blood-water partition coefficient, calculated according to Fitzsimmons et al. 2001:

$$P_{BW} = \left(\left(10^{0.73\log Kow} \times 0.16\right) + 0.84\right) \quad (6)$$

It was shown previously that Eqn. 6 provides reasonable estimates of ϕ_P when compared to blood binding data for chemicals covering an extensive log K_{OW} range (Nichols et al. 2013b).

The ϕ_{S9} was estimated using algorithms given by Han et al. 2009, Nichols et al. 2017, and Lee et al. 2017. The empirical relationship given by Han et al. 2009 was originally developed using binding data for rat liver microsomes, but has been incorporated in current IVIVE approaches (Nichols et al. 2013b) to describe the unbound chemical fraction in trout liver S9 as a function of chemical log K_{OW} and S9 protein content (C_{S9}; mg mL^{-1}):

$$\phi_{S9;\ Han} = 1/\left(C_{S9} \times 10^{0.694\log Kow - 2.158} + 1.0\right) \quad (7)$$

More recently Nichols et al. 2017 measured unbound chemical fractions for 3 polycyclic aromatic hydrocarbons (PAH) in rainbow trout S9 using a vial equilibration method, and derived a general equation to estimate chemical binding:

$$\phi_{S9;\,Nichols} = 1/\left(C_{S9} \times 10^{1.33\log Kow - 4.6} + 1.0\right) \quad (8)$$

The tissue-composition based algorithm given by Lee et al. 2017 estimates $\phi_{,S9}$ based on fractional amounts of lipid and non-lipid organic matter (protein) in the incubation medium:

$$\phi_{s9;Lee} = F_{W,S9}/\left(F_{L,S9}K_{OW} + F_{P,S9}\beta K_{OW} + F_{W,S9}\right) \quad (9)$$

where $F_{W,S9}$, $F_{L,S9}$, and $F_{P,S9}$ are the fractions of water, lipid, and protein (v/v; unitless), respectively. The proportionality constant (β) reflects the sorptive capacity of protein relative to that of octanol and was assumed to be 0.05 (deBruyn & Gobas 2007). Measured values of $F_{L,S9}$ and $F_{P,S9}$ determined in the present study are provided in Table S2.

Unbound fractions determined using Eqn. 7–9 were employed as inputs to the well-stirred liver model to evaluate the effects of estimated S9 binding on calculated levels of CL_H, and by extension modeled BCFs. Additional estimates of CL_H were obtained under the assumption that $\phi_{S9} = \phi_P$ (i.e. f_U=1.0), as previous work suggests that chemical bioavailability to metabolizing enzymes in S9 and blood plasma is effectively the same (Nichols et al. 2013a; Laue et al. 2014). *In vivo* biotransformation rate constants (k_{MET}; d^{-1}) were calculated by dividing CL_H by the chemical's apparent volume of distribution (V_D; L kg^{-1}). The V_D relates the sorptive capacity of the fish to that of blood at steady state, and was calculated as: ($v_{L,WB}$ K_{OW})/P_{BW}, where v_{LWB} is the fractional lipid content of the organism (0.05). Parameters and equations contained within the IVIVE model are displayed in Table S3 of the Supplemental Data.

The model used to describe chemical bioaccumulation in fish may be written as (Arnot & Gobas 2004):

$$\frac{dc_f}{dt} = \left(k_1 \times C_{WT}\phi\right) - \left(k_2 + k_E + k_{MET} + k_G\right) \times C_F \quad (10)$$

where C_F is the concentration of chemical in the fish (g kg^{-1}); t is time (d); k_1 is the mass and volume specific rate constant for uptake from respired water (L kg^{-1} d^{-1}); C_{WT} is the total concentration of chemical in the water (g L^{-1}); ϕ is the bioavailable solute fraction (unitless); and k_2, k_E, k_{MET}, and k_G are first-order rate constants (d^{-1}) representing chemical elimination from the fish by passive diffusion across gills, fecal egestion, metabolic biotransformation, and growth dilution, respectively. Parameters and equations contained within the model are provided in Table S4 of the Supplemental Data.

RESULTS AND DISCUSSION

Characterization of UVF biotransformation reactions in vitro

No significant depletion of any UVF was observed in assays with heat-treated S9 (Figure 2). 4-MBC was not significantly depleted in active S9 fractions without cofactors, suggesting negligible contribution of cofactor-independent enzymes (p=0.98; Figure 2, Panel A). *In vitro* biotransformation of 4-MBC was entirely dependent on the addition of NADPH, as the mean k_{dep} measured in S9 with added NADPH did not differ from the mean k_{dep} measured in S9 fractions with added NADPH and phase II cofactors (p=0.22). This finding is indicative of the involvement of one or more CYPs. Previous work has shown that rats rapidly metabolize 4-MBC and that this activity involves CYP-mediated oxidation reactions (Völkel et al. 2006).

Significant depletion of EHMC was observed in the absence of NADPH (p=0.01; Figure 2, Panel B). The addition of NADPH resulted in maximal rates of activity for EHMC; the mean k_{dep} did not significantly differ between incubations containing NADPH and those with NADPH and phase II cofactors (p=0.18). NADPH addition had no apparent impact on the metabolism of OCT, as the k_{dep} values measured for OCT were statistically similar in all active S9 fractions both with and without NADPH (p=0.49; Figure 2; Panel C). These findings suggest that hydrolysis of EHMC and OCT by carboxylesterases is an important route of metabolism. Carboxylesterases do not require cofactors and are active in rainbow trout liver (Barron et al. 1999; Butt et al. 2010). Biotransformation of EHMC in rodents proceeds exclusively through initial hydrolysis of the ester bond (Fennell et al. 2017). If hydrolysis is the primary biotransformation pathway for EHMC in trout, our findings suggest that both CYP enzymes and carboxylesterases may catalyze this activity (Guengerich 1987). Identification of UVF metabolites would provide additional insight to the pathways involved in UVF biotransformation. Addition of the phase II cofactors GSH, PAPs, and UDPGA did not affect depletion rates of 4-MBC, EHMC, or OCT, suggesting that phase II conjugation enzymes do not act directly on these UVFs. Phase II cofactors were therefore excluded from all subsequent depletion experiments.

Concentration dependence of UVF in vitro depletion rate constants

Depletion studies with EHMC and OCT were conducted across a range of initial concentrations with and without added NADPH to obtain kinetic parameters for these two incubation mixtures. For 4-MBC, only incubations with added NADPH were performed (Figure 3). The rate of UVF depletion decreased with increasing initial concentration. Fitted k_{dep} values for each UVF exhibited a sigmoidal relationship with initial substrate concentration, consistent with Eqn. 2 (Figure 4). The inflection point of each fitted relationship (dashed lines) represents the apparent K_m value for the reaction. Kinetic parameters for each UVF are given in Table 2.

Initial findings did not suggest an effect of NADPH addition on the *in vitro* depletion of OCT (Figure 2, Panel C); however, studies with multiple concentrations of OCT (Figure 4, Panel C) revealed a contribution of both NADPH independent and dependent activity. The

failure of earlier work to show an effect of NADPH may have been due to the variance in the k_{dep} measured at a single concentration.

The $CL_{in\ vitro,\ int}$ measured for 4-MBC was significantly greater (7 to 25-fold) than values obtained for EHMC or OCT. This finding can be attributed in part to a lower K_m and higher estimated V_{max} for 4-MBC, compared to values determined for EHMC and OCT. Using the described methods, however, V_{max} is a dependent variable, calculated as $CL_{in\ vitro,\ int} \times K_m$. Interpretation of V_{max} is therefore complicated by the possibility of errors in measurement of $CL_{in\ vitro,\ int}$, estimation of K_m, or both. For EHMC and OCT, addition of NADPH resulted in modest (2-fold) increases in $CL_{in\ vitro,\ int}$, which were associated with corresponding increases in V_{max}. Kinetic constants determined for EHMC and OCT in the absence of NADPH may represent a single reaction pathway catalyzed by a carboxylesterase. In contrast, metabolism of EHMC and OCT in the presence of NADPH almost certainly involves more than one enzyme, possibly including both a CYP and a carboxylesterase.

The IVIVE approach assumes that *in vitro* activity is measured under near non-saturating conditions. By testing over a range of *in vitro* substrate concentrations, it is possible to confirm that this assumption has been met. The derived K_m value for 4-MBC was 0.29 μM, and overall 3 of the 5 determined K_m values were < 1.0 μM. In previous studies, the IVIVE approach has been applied using *in vitro* data collected at initial concentrations ≥1.0 μM. More recent work, conducted using trout liver S9 fractions, has shown that K_m values for several polycyclic aromatic hydrocarbons (PAHs) are substantially lower than 1.0 μM. For example, Lo et al. 2015a obtained K_m values of 0.14 μM, 0.18 μM, and 0.31 μM for chrysene, benzo(a)pyrene, and pyrene, respectively. In a similar study, Nichols et al. 2017 reported K_m values of 0.52 μM, 0.07 μM, and 0.03 μM for phenanthrene, pyrene, and benzo(a)pyrene, respectively. The present work is consistent, therefore, with recent studies on PAHs, and suggests that an initial concentration ≥1.0 μM may exceed the K_m value for many hydrophobic substrates.

Use of the IVIVE method to inform bioaccumulation models also depends on the existence of first-order reaction conditions in fish under field conditions. To test this assumption, lipid-normalized concentrations of UVFs in fish were compared to lipid-normalized K_m values measured in the present study (Table 2). Measured concentrations of 4-MBC, EHMC, and OCT in field-collected fish range between 0.11 to 1.42 nmol g lipid^{-1} (Gago-Ferrero et al. 2012) and are 2 orders of magnitude lower than the lipid normalized K_m values presented here. This finding suggests that for these chemicals the metabolic pathways in field-collected fish operate under non-saturating conditions and that extrapolated *in vivo* biotransformation potential is better represented by $k_{dep,C\rightarrow 0}$ than by the k_{dep} measured at initial concentrations

of ≥1.0 μM.

Fraction unbound in the incubation medium

Binding correction factors ($f_U = \phi_P/\phi_{S9}$) used to extrapolate *in vitro* data to the intact tissue can have large impacts on IVIVE-estimated biotransformation rates and BCFs (Nichols et al. 2013b; Laue et al. 2014). Because there is considerable uncertainty in the determination of

ϕ_{S9}, available S9 binding algorithms (Eqn. 7 to 9) were evaluated. Chemical bound/free ratios estimated using Eqn. 7 to 9 increased linearly with chemical log K_{OW} (Figure 5), but these estimates diverged substantially at log $K_{OW} > 5$ due to differences in slope terms between the available algorithms. In earlier studies, it was assumed that the unbound chemical fraction in fish liver S9 was the same as in rat liver microsomes (Han et al. 2009). More recently, Nichols et al. developed a binding algorithm using measured data for 3 PAHs in trout S9 fractions. At log $K_{OW} > 5$, this algorithm estimates substantially greater binding than the $\phi_{S9;\ Han}$ algorithm (Nichols et al. 2017). This disparity may be due to differences in the composition of liver S9 and microsomal systems. Procedures used to isolate liver microsomes begin with isolation of the S9 fraction, but include two additional high-speed centrifugation steps and a wash/reconstitution step that are likely to remove residual non-polar lipid. Species differences between rat and trout may also contribute to differences between the two binding models.

An examination of available empirical ϕ_{S9} data for trout indicates that measured bound/free ratios in S9 (normalized to 2 mg protein mL^{-1}) also vary substantially (Figure 4). For example, values given for pyrene (log $K_{OW} = 4.88$) vary 10-fold while those reported for benzo(a)pyrene (log $K_{OW} = 6.13$) vary by 100-fold. This variation may be due in part to the use of different measurement methods. Equilibrium dialysis is widely employed to study chemical binding, but this technique is difficult to use when unbound chemical fractions are extremely low (< 0.1%). Nichols et al. measured the extent of S9 binding using both solid phase microextraction (Nichols et al. 2013a) and a vial equilibration technique (Nichols et al. 2017). Unbound chemical fractions have also been measured using a thin-film sorbent (ethylene vinyl acetate) phase dosing system (Lee et al. 2014; Lo et al. 2015). Liver S9 binding measurements reported by Escher et al. 2011 were obtained using a polydimethylsiloxane (PDMS) depletion method. Standardized methods for measuring ϕ_{S9} may help to reduce variability in the experimental binding data and lead to improved binding algorithms. Uncertainty in the determination of ϕ_{S9} greatly impacts the extrapolation of *in vitro* biotransformation rates to generate modeled BCFs, and may explain apparent discrepancies between empirical BCFs and BCFs calculated by IVIVE procedures. The effect of chemical binding on hepatic clearance remains a principal source of uncertainty in the extrapolation of biotransformation rates in fish (Laue et al. 2014).

Modeled bioconcentration factors

Modeled BCFs for each UVF illustrate how differences in *in vitro* activity at different initial concentrations, when combined with different estimates of ϕ_{S9}, can yield different estimates of bioconcentration (Figure 6). Because the calculation of f_U considers unbound chemical fractions in both blood plasma and S9, different ϕ_{S9} values estimated using Eqn. 7 to 9 produced different f_U values (Table 3). In this evaluation, ϕ_P was assumed correct and left constant as previous work suggests that Eqn. 6 provides reasonable estimates of ϕ_P when compared to empirical data (Nichols et al. 2013b). Individual panels in Figure 6 show the range of empirical BCFs for each UVF, the REACH criterion for bioaccumulative substances (BCF > 2000 L kg^{-1}), the measured K_m value for the reactions, and the BCFs calculated assuming no biotransformation ($k_{dep} = 0$ min^{-1}). These latter values are approximately 4000, 17600, and 17200 L kg^{-1} for 4-MBC, EHMC, and OCT, respectively.

Modeled BCFs for 4-MBC, EHMC, and OCT decreased with decreasing initial test concentration in the incubation medium at each assumed level of binding, and approached a minimum value at initial test concentrations well below K_m. For each UVF, however, differences in BCFs calculated at concentrations below K_m were relatively small (< 50%), suggesting that it may be possible to establish guidance (e.g., $\leq 1/10^{th}$ K_m) regarding test concentrations that would be required to yield high-quality BCF predictions.

The apparent *in vitro* concentration dependence of modeled BCFs may also help explain the tendency of IVIVE methods to overestimate BCFs relative to empirical data (Han et al. 2009; Laue et al. 2014). The past use of substrate concentrations ranging from 1 to 10 μM (Han et al. 2007; Cowan-Ellsberry et al. 2008; Johanning et al. 2012) may have saturated biotransformation enzymes, resulting in underestimates of k_{MET} and overestimates of the BCF. In the present study, BCFs calculated from both $k_{dep,C\rightarrow 0}$ and the k_{dep} measured at initial concentrations of 0.05 μM were up to 2-fold and 7-fold lower than those generated from reaction rates measured at 1 μM and 10 μM, respectively.

Differences in the estimated ϕ_{S9} values resulted in different BCFs for a fixed level of *in vitro* activity; but the extent of these differences depended on the rate of biotransformation. For example, all BCFs for 4-MBC (Figure 6, Panel A) fell below the BCF criterion of 2000 L kg^{-1}. This is due to 4-MBC's rapid *in vitro* biotransformation. Moreover, k_{dep} values measured at concentrations ≤ 1 μM resulted in BCFs that differed less than 2-fold under all binding scenarios. The similarity of these modeled BCFs can be attributed to the behavior of the well-stirred liver model (Eqn. 3). When intrinsic clearance rates are high, hepatic clearance becomes rate-limited by blood flow to the liver, resulting in modeled hepatic clearance that is relatively insensitive to changes in f_U (Laue et al. 2014). When intrinsic clearance rates are low, competing binding assumptions can result in substantial differences in calculated hepatic clearance rates, and by extension modeled BCFs (Nichols et al. 2013b). The BCFs calculated for EHMC and OCT were much more sensitive to differences in f_u across all tested concentrations, including those well below K_m. Measured $CL_{in\ vitro,\ int}$ rates for EHMC and OCT were approximately one order of magnitude lower than that determined for 4-MBC (Table 2).

Using the $\phi_{S9;\ Han}$ algorithm, the k_{dep} measured at an initial concentrations of 1 μM, resulted in modeled BCFs of approximately 2400 L kg^{-1} and 2500 L kg^{-1} for EHMC and OCT, respectively, exceeding the REACH criterion for bioaccumulative substances (Figure 6; Panels B and C). At the same tested concentrations, the $\phi_{S9;\ Nichols}$ and $\phi_{S9;\ Lee}$ algorithms resulted in BCFs well below 2000 L kg^{-1}. Using the $k_{dep,C\rightarrow 0}$, all modeled BCFs fell below the REACH criterion, ranging from 324 to 1578 L kg^{-1} for EHMC and from 177 to 1914 L kg^{-1} for OCT. When interpreted in the context of chemical concentrations likely to exist in fish under field conditions, these findings suggest that bioaccumulation (BCF ≥ 2000 L kg^{-1}) of EHMC and OCT is unlikely. The empirical BCF data for these chemicals, determined in *in vivo* laboratory experiments, are also consistent with this suggestion (Figure 6).

This investigation highlights the need for further refinement of the f_U calculation. Uncertainty in the determination of ϕ_{S9} greatly impacts the extrapolation of *in vitro*

biotransformation rates to generate modeled BCFs (Figure 6). While the available binding algorithms may be appropriate for screening-level assessments, high quality estimates of f_U will require additional empirical ϕ_{S9} and ϕ_P data for a range of chemicals, representing different chemical classes. Additionally, the present investigation assumed that ϕ_P estimates were correct, yet this assumption may itself be incorrect. Several of the f_U values calculated in this study approached or exceeded 1.0 (Table 3). The lipid and protein content of trout plasma (1.84 and 4.12 %, respectively (Escher et al. 2011)) is substantially higher than that of liver S9 fractions (measured here (Table S2) and elsewhere (Escher et al. 2011)). Absent specific binding, it would be reasonable to expect that ϕ_P would be substantially lower than ϕ_{S9}, producing f_U estimates of less than 1.0. Using the same PDMS depletion method, Escher et al. 2011 obtained ϕ_{S9} and ϕ_P data for several hydrophobic chemicals (log K_{OW} 4.5 to 5.1). Resulting f_U values ranged from 0.0042 to 0.02333 indicating that ϕ_P is up to 240 times lower than ϕ_{S9}. These findings may have been impacted, however, by heat-treatment of the S9 sample to eliminate metabolic activity. Others have found that binding measurements may be made using S9 samples inactivated by time and the absence of cofactors (Nichols et al. 2017).

Finally, there is some reason to question whether the steady-state assumption represented by use of the f_U binding term is appropriate. In the present study, setting $f_U = 1.0$ resulted in BCFs that fell within or slightly below the range of empirical values for most of the modeled conditions. Several authors have reported that BCFs calculated using *in vitro* biotransformation data exhibited improved agreement with empirical data when f_U was set to 1.0 (Escher et al. 2011; Laue et al. 2014). One explanation for these findings is that bound chemicals rapidly dissociate from molecular binding sites in plasma, making them available for metabolism in the time available for this activity to occur (i.e., the residence time of blood in the liver (Escher et al. 2011; Nichols et al. 2013b)). This or a similar kinetic process may also help explain the observed trend toward overestimation of measured BCFs by current IVIVE methods (i.e., when $f_U = \phi_P/\phi_{S9}$), and would require development of a more sophisticated model to estimate hepatic clearance rates from measured k_{dep} values.

Summary and conclusions

The present study highlights the importance of using appropriate *in vitro* test concentrations and f_U binding correction factors when using extrapolated *in vitro* biotransformation rates to refine modeled BCFs. Previously, it was suggested that use of different binding terms (including $f_U = 1.0$) may be appropriate to estimate upper and lower limits of hepatic clearance, generating a range of BCFs (Nichols et al. 2013b; Laue et al. 2014). The use of multiple *in vitro* test concentrations could also provide a conservative assessment when evaluating chemical bioaccumulation potential in fish. For example, if the highest measured rate of biotransformation does not reduce the BCF below a regulatory criterion, lower levels of activity would only result in higher estimates (Nichols et al. 2017). This type of information could complement weight-of-evidence approaches that have been advocated for in chemical bioaccumulation assessments (Weisbrod et al. 2009). When these factors are taken into consideration, the data in this study indicate that 4-MBC, EHMC, and OCT are metabolized by trout at rates high enough to reduce bioconcentration below existing criteria.

Additional data are needed to determine whether other fish species metabolize these UVFs, although BCFs measured for other species are suggestive of this.

Supplementary Material

Refer to Web version on PubMed Central for supplementary material.

Acknowledgement –

REFERENCES

Arnot JA, Gobas FAPC. 2006 A review of bioconcentration factor (BCF) and bioaccumulation factor (BAF) assessments for organic chemicals in aquatic organisms. Environ Rev. 14:257–297.

Arnot JA, Gobas FAPC. 2004 A food web bioaccumulation model for organic chemicals in aquatic ecosystems. Environ Tox Chem. 23:2343–2355.

Arnot JA, Mackay D, Bonnell M. 2008 Estimating metabolic biotransformation rates in fish from laboratory data. Environ Tox Chem. 27:341–351.

Arnot JA, Meylan W, Tunkel J, Howard PH, Mackay D, Bonnell M, Boethling RS. 2009 A quantitative structure-activity relationship for predicting metabolic biotransformation rates for organic chemicals in fish. Environ Tox Chem. 28:1168–1177.

Bachelot M, Li Z, Munaron D, Le Gall P, Casellas C, Fenet H, Gomez E. 2012 Organic UV filter concentrations in marine mussels from French coastal regions. Sci Total Environ. 420:273–279. [PubMed: 22330425]

Balmer ME, Buser H-R, Müller MD, Poiger T. 2005 Occurrence of some organic UV Filters in wastewater, in surface waters, and in fish from Swiss lakes. Environ Sci Technol. 39:953–962. [PubMed: 15773466]

Barron MG, Charron KA, Stott WT. 1999 Tissue carboxylesterase activity of rainbow trout. Environ Tox Chem. 18:2506–2511.

Bligh EG, Dyer WJ. 1959 A rapid method of total lipid extraction and purification. Can J Biochem Phys. 37:911–917.

Blüthgen N, Meili N, Chew G, Odermatt A, Fent K. 2014 Accumulation and effects of the UV-filter octocrylene in adult and embryonic zebrafish (Danio rerio). Sci Total Environ. 476–477:207–217.

Bradford MM. 1976 A rapid and sensitive method for the quantitation of microgram quantities of protein utilizing the principle of protein-dye binding. Anal Biochem. 72:248–254. [PubMed: 942051]

Buser H-R, Balmer ME, Schmid P, Kohler M. 2006 Occurrence of UV Filters 4-methylbenzylidene camphor and octocrylene in fish from various Swiss rivers with inputs from wastewater treatment plants. Environ Sci Technol. 40:1427–1431. [PubMed: 16568752]

Butt CM, Muir DCG, Mabury SA. 2010 Biotransformation of the 8:2 fluorotelomer acrylate in rainbow trout. 2. In vitro incubations with liver and stomach S9 fractions. Environ Tox Chem. 29:2736–2741.

Connors KA, Du B, Fitzsimmons PN, Hoffman AD, Chambliss CK, Nichols JW, Brooks BW. 2013 Comparative pharmaceutical metabolism by rainbow trout (Oncorhynchus mykiss) liver S9 fractions. Environ Tox Chem. 32:1810–1818.

Cowan-Ellsberry CE, Dyer SD, Erhardt S, Bernhard MJ, Roe AL, Dowty ME, Weisbrod AV. 2008 Approach for extrapolating in vitro metabolism data to refine bioconcentration factor estimates. Chemosphere. 70:1804–1817. [PubMed: 17904615]

deBruyn A, Gobas FAPC. 2007 The sorptive capacity of animal protein. Environ Tox Chem. 26:1803–1808.

Escher BI, Cowan-Ellsberry CE, Dyer S, Embry MR, Erhardt S, Halder M, Kwon J-H, Johanning K, Oosterwijk MTT, Rutishauser S, Segner H, Nichols JW. 2011 Protein and lipid binding parameters in rainbow trout (Oncorhynchus mykiss) blood and liver fractions to extrapolate from an in vitro metabolic degradation assay to in vivo bioaccumulation potential of hydrophobic organic chemicals. Chem Res Toxicol. 24:1134–1143. [PubMed: 21604782]

Fay KA, Fitzsimmons PN, Hoffman AD, Nichols JW. 2016 Comparison of trout hepatocytes and liver S9 fractions as in vitro models for predicting hepatic clearance in fish. Environ Tox Chem. 36:463–471.

Fennell TR, Mathews JM, Snyder RW, Hong Y, Watson SL, Black SR, McIntyre BS, Waidyanatha S. 2017 Metabolism and disposition of 2-ethylhexyl- p-methoxycinnamate following oral gavage and dermal exposure in Harlan Sprague Dawley rats and B6C3F1/N mice and in hepatocytes in vitro. Xenobiotica, in press. DOI: 10.1080/00498254.2017.1400129

Fent K, Weston AA, Caminada D. 2006 Ecotoxicology of human pharmaceuticals. Aquat Sci. 76:122–159.

Fent K, Zenker A, Rapp M. 2010 Widespread occurrence of estrogenic UV-filters in aquatic ecosystems in Switzerland. Environ Pollut. 158:1817–1824. [PubMed: 20004505]

Fitzsimmons PN, Fernandez JD, Hoffman AD, Butterworth BC, Nichols JW. 2001 Branchial elimination of superhydrophobic organic compounds by rainbow trout (Oncorhynchus mykiss). Aquat Toxicol. 55:23–34. [PubMed: 11551619]

Gago-Ferrero P, Alonso MB, Bertozzi CP, Marigo J, Barbosa L, Cremer M, Secchi ER, Domit C, Azevedo A, Lailson-Brito J, et al. 2013 First determination of UV filters in marine mammals. Octocrylene levels in Franciscana dolphins. Environ Sci Technol. 47:5619–5625. [PubMed: 23627728]

Gago-Ferrero P, Díaz-Cruz MS, Barceló D. 2012 An overview of UV-absorbing compounds (organic UV filters) in aquatic biota. Anal Bioanal Chem. 404:2597–2610. [PubMed: 22669305]

Gago-Ferrero P, Díaz-Cruz MS, Barceló D. 2015 UV filters bioaccumulation in fish from Iberian river basins. Sci Total Environ, 518–519:518–525.

Gobas FAPC, de Wolf W, Burkhard LP, Verbruggen E, Plotzke. 2009 Revisiting bioaccumulation criteria for POPs and PBT assessments. Integr Environ Assess Manag. 5:624–637. [PubMed: 19552497]

Guengerich FP. 1987 Oxidative cleavage of carboxylic esters by cytochrome P-450. J Biol Chem. 262:8459–8462. [PubMed: 3597381]

Han X, Nabb DL, Mingoia RT, Yang C-H. 2007 Determination of xenobiotic intrinsic clearance in freshly isolated hepatocytes from rainbow trout (Oncorhynchus mykiss) and rat and its application in bioaccumulation assessment. Environ Sci Technol. 41:3269–3276. [PubMed: 17539536]

Han X, Nabb DL, Yang C-H, Snajdr SI, Mingoia RT. 2009 Liver microsomes and S9 from rainbow trout (Oncorhynchus mykiss): Comparison of basal level enzyme activities with rat and determination of xenobiotic intrinsic clearance in support of bioaccumulation assessment. Environ Tox Chem. 28:481–488.

Johanning K, Hancock G, Escher B, Adekola A, Bernhard MJ, Cowan-Ellsberry C, Domoradzki J, Dyer S, Eickhoff C, Embry M, Erhardt S, Fitzsimmons P, Halder M, Hill J, Holden D, Johnson R, Rutishauser S, Segner H, Schultz R, Nichols J. 2012 Assessment of metabolic stability using the rainbow trout (Oncorhynchus mykiss) liver S9 fraction. Curr Protoc Toxicol. 1410:1–28.

Laue H, Gfeller H, Jenner KJ, Nichols JW, Kern S, Natsch A. 2014 Predicting the bioconcentration of fragrance ingredients by rainbow trout using measured rates of in vitro intrinsic clearance. Environ Sci Technol. 48:9486–9495. [PubMed: 25058173]

Lee Y-S, Lee DHY, Delafoulhouze M, Otton SV, Moore MM, Kennedy CJ, Gobas FAPC. 2014 In vitro biotransformation rates in fish liver S9: Effect of dosing techniques. Environ Tox Chem. 33:1885–1893.

Lee Y-S, Lo JC, Otton SV, Moore MM, Kennedy CJ, Gobas FAPC. 2017 In vitro to in vivo extrapolation of biotransformation rates for assessing bioaccumulation of hydrophobic organic chemicals in mammals. Environ Tox Chem. 36:1934–1946.

Li VWT, Tsui MPM, Chen X, Hui MNY, Jin L, Lam RHW, Yu RMK, Murphy MB, Cheng J, Lam PKS, Cheng SH. 2016 Effects of 4-methylbenzylidene camphor (4-MBC) on neuronal and muscular development in zebrafish (Danio rerio) embryos. Env Sci Poll Res. 23:8275–8285.

Lo JC, Allard GN, Otton SV, Campbell DA, Gobas FAPC. 2015 Concentration dependence of biotransformation in fish liver S9: Optimizing substrate concentrations to estimate hepatic clearance for bioaccumulation assessment. Environ Tox Chem. 34:2782–2790.

Lo JC, Campbell DA, Kennedy CJ, Gobas FAPC. 2015 Somatic and gastrointestinal in vivo biotransformation rates of hydrophobic chemicals in fish. Environ Tox Chem. 34:2282–2294.

Lo JC, Letinski DJ, Parkerton TF, Campbell DA, Gobas FAPC. 2016 In vivo biotransformation rates of organic chemicals in fish: Relationship with bioconcentration and biomagnification factors. Environ Sci Technol. 50:13299–13308. [PubMed: 27993034]

Mingoia RT, Glover KP, Nabb DL, Yang C-H, Snajdr SI, Han X. 2010 Cryopreserved hepatocytes from rainbow trout (Oncorhynchus mykiss): a validation study to support their application in bioaccumulation assessment. Environ Sci Technol. 44:3052–3058. [PubMed: 20196591]

Nagtegaal M, Ternes TA, Baumann W, Nagel R. 1997 UV-filtersubstanzen in wasser und fischen. UWSF. 9:79–86.

Nath A, Atkins WM. 2006 A theoretical validation of the substrate depletion approach to determining kinetic parameters. Drug Metab Dispos. 34:1433–1435. [PubMed: 16751261]

Nichols JW, Bonnell M, Dimitrov SD, Escher BI, Han X, Kramer NI. 2009 Bioaccumulation assessment using predictive approaches. Integr Environ Assess Manag. 5:577–597. [PubMed: 19775192]

Nichols JW, Hoffman AD, Laak ter TL, Fitzsimmons PN. 2013 Hepatic clearance of 6 polycyclic aromatic hydrocarbons by isolated perfused trout livers: Prediction from in vitro clearance by liver S9 fractions. Toxicol Sci. 136:359–372. [PubMed: 24097670]

Nichols JW, Huggett DB, Arnot JA, Fitzsimmons PN, Cowan-Ellsberry CE. 2013 Towards improved models for predicting bioconcentration of well-metabolized compounds by rainbow trout using measured rates of in vitro intrinsic clearance. Environ Tox Chem. 32:1611–1612.

Nichols JW, Ladd MA, Fitzsimmons PN. 2017 Measurement of kinetic parameters for biotransformation of polycyclic aromatic hydrocarbons by trout liver S9 fractions: Implications for bioaccumulation assessment. Appl In Vitro Toxicol, in press. DOI: 10.1089/aivt.2017.0005

Nichols JW, Schultz IR, Fitzsimmons PN. 2006 In vitro-in vivo extrapolation of quantitative hepatic biotransformation data for fish. I. A review of methods, and strategies for incorporating intrinsic clearance estimates into chemical kinetic models. Aquat Toxicol. 78:74–90. [PubMed: 16513189]

Obach RS, Reed-Hagen AE. 2002 Measurement of michaelis constants for cytochrome P450-mediated biotransformation reactions using a substrate depletion approach. Drug Metab Dispos. 30:831–837. [PubMed: 12065442]

Picot Groz M, Martinez Bueno MJ, Rosain D, Fenet H, Casellas C, Pereira C, Maria V, Bebianno MJ, Gomez E. 2014 Detection of emerging contaminants (UV filters, UV stabilizers and musks) in marine mussels from Portuguese coast by QuEChERS extraction and GC-MS/MS. Sci Total Environ. 493:162–169. [PubMed: 24946029]

Sigma-Aldrich. 2014 Safety Data Sheet: 2-Ethylhexyl 2-cyano-3,3-diphenylacrylate [Cited 2017 Sept 23] Available from: https://www.sigmaaldrich.com/catalog/product/aldrich/415820

Sijm D, Opperhuizen A. 1989 Biotransformation rates of xenobiotic compounds in relation to enzymes activities: A critical review. Toxicol Environ Chem. 23:181–190.

Sijm DT, Yarechewski AL, Muir DC, Webster GB, Seinen W, Opperhuizen A. 1990 Biotransformation and tissue distribution of 1,2,3,7-tetrachlorodibenzo-p-dioxin, 1,2,3,4,7-pentachlorodibenzo-p-dioxin and 2,3,4,7,8-pentachlorodibenzofuran in rainbow trout. Chemosphere. 21:845–866.

Trowell JJ, Frank A. Gobas PC, Moore MM, Kennedy CJ. 2018 Estimating the bioconcentration factors of hydrophobic organic compounds from biotransformation rates using rainbow trout hepatocytes. Arch Environ Contam Toxicol. 75: 295–305. [PubMed: 29550936]

US National Library of Medicine. 2006 TOXNET Hazardous Substances Data Bank. Washington, DC [cited 2017 April 30]. Available from: https://toxnet.nlm.nih.gov/newtoxnet/hsdb.htm

van den Heuvel MR, Dixon DG, Munkittrick KR, Stegeman JJ. 1995 Second-round interlaboratory comparison of hepatic ethoxyresorufin-O-deethylase activity in white sucker (Catostomus commersoni) exposed to bleached-kraft pulp mill effluent. Envon Tox Chem. 14:1513–1320.

Völkel W, Colnot T, Schauer UMD, Broschard TH, Dekant W. 2006 Toxicokinetics and biotransformation of 3-(4-methylbenzylidene)camphor in rats after oral administration. Toxicol Appl Pharmacol. 216:331–338. [PubMed: 16806338]

Weisbrod AV, Woodburn KB, Koelmans AA, Parkerton TF, McElroy AE, Borgå K. 2009 Evaluation of bioaccumulation using in vivo laboratory and field studies. Integr Environ Assess Manag. 5:598–623. [PubMed: 19552500]

Wilkinson GR, Shand DG. 1975 Commentary: A physiological approach to hepatic drug clearance. Clin Pharmacol Ther. 18:377–390. [PubMed: 1164821]

Zenker A, Schmutz H, Fent K. 2008 Simultaneous trace determination of nine organic UV-absorbing compounds (UV filters) in environmental samples. J Chromatogr A. 1202:64–74. [PubMed: 18632108]
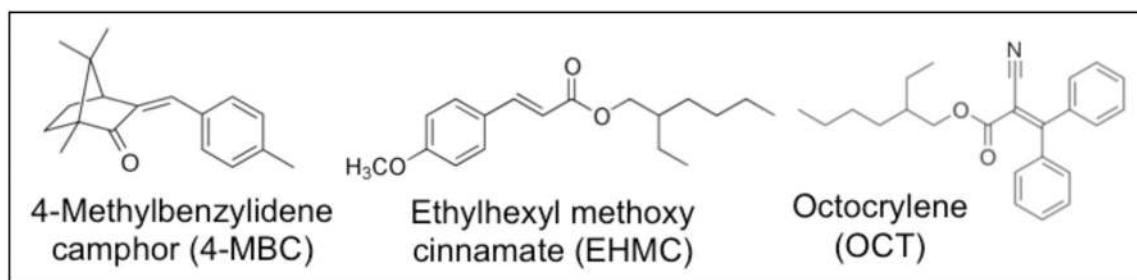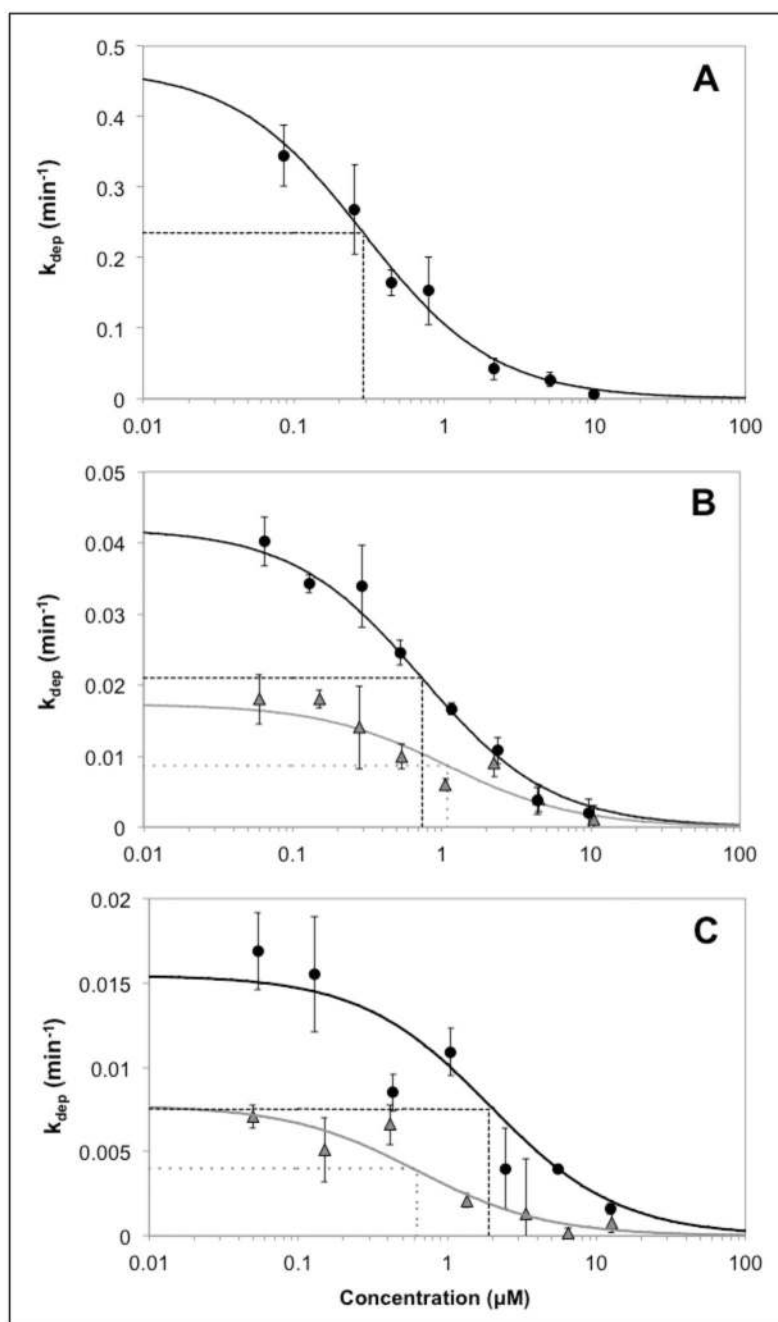
Figure 1.
Structures, names, and abbreviations of 4-methylbenzylidene (4-MBC), 2-ethylhexyl-4-methoxycinnamate (EHMC), and octocrylene (OCT).
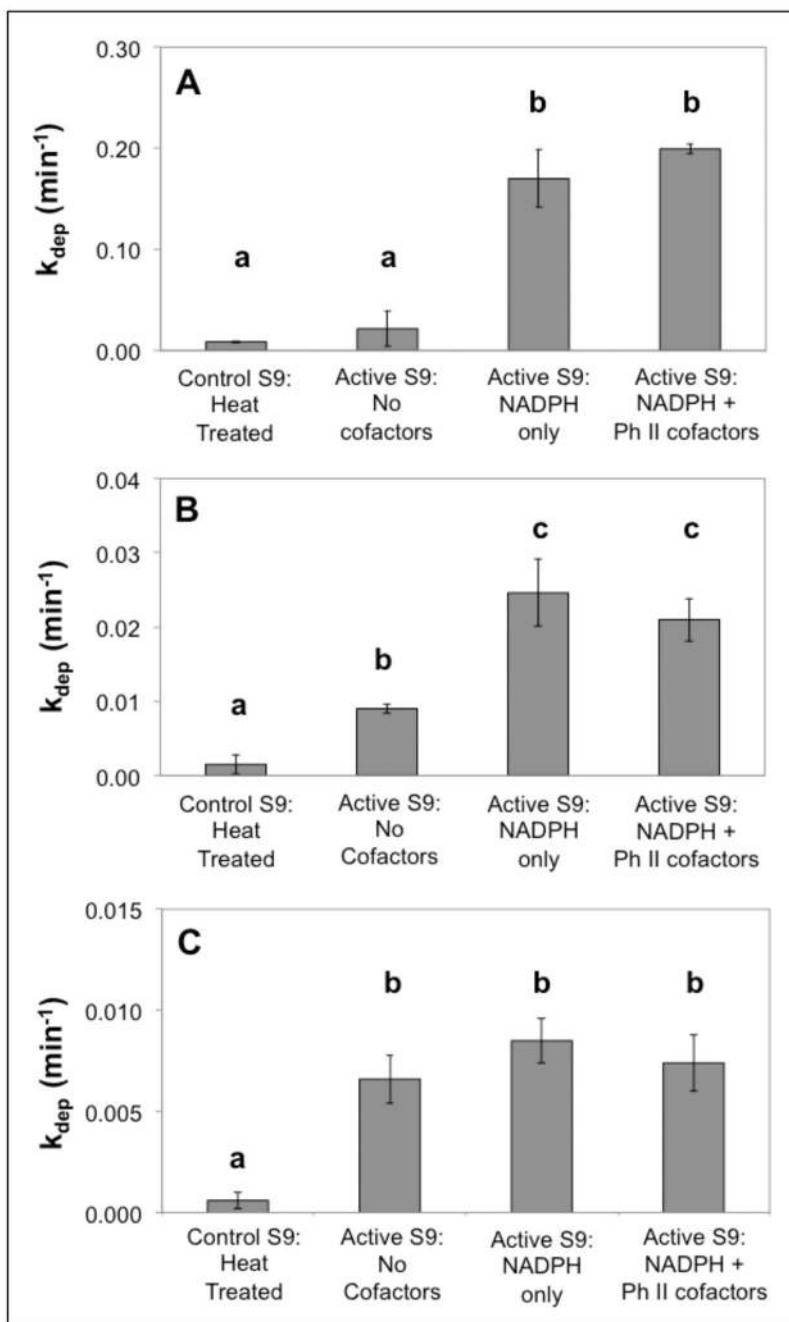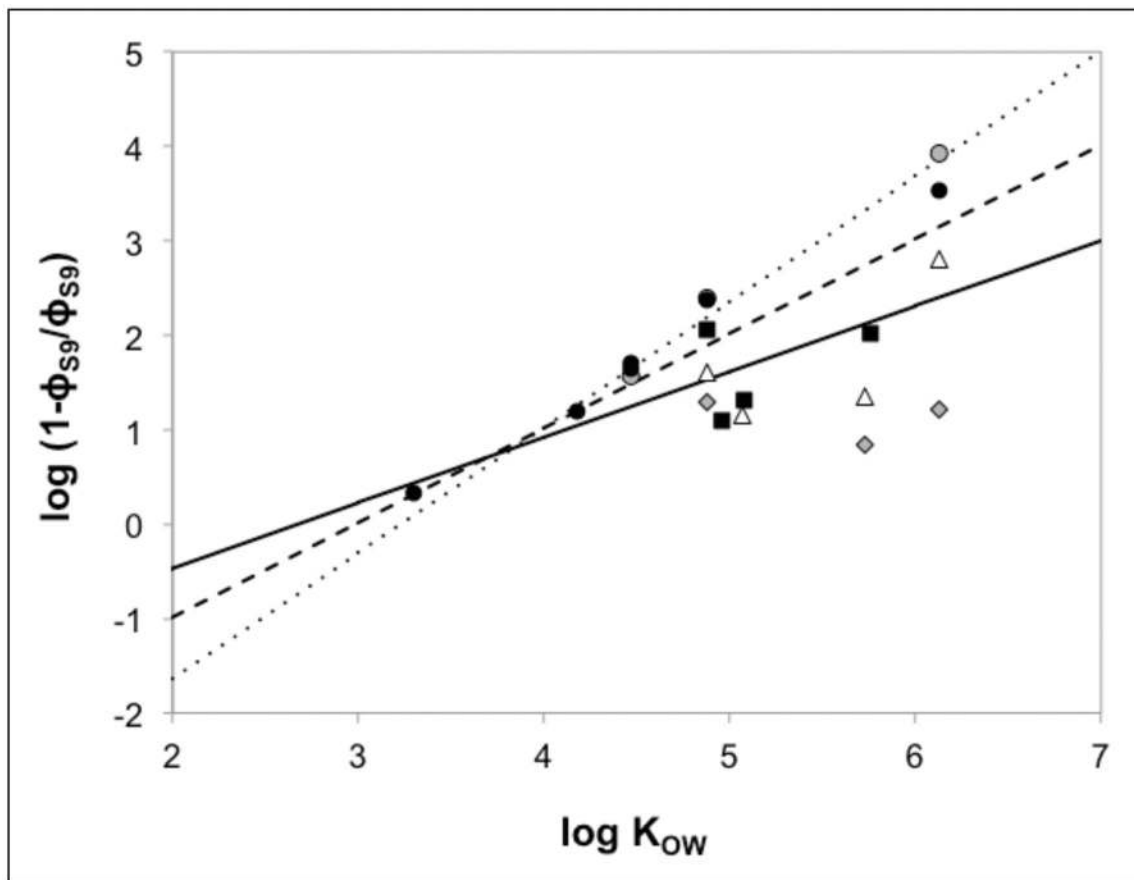
Figure 2.
Mean *in vitro* biotransformation rate constants (k_{dep}) for 0.5 μM 4-MBC (A), 0.5 μM EHMC (B), and 0.5 μM OCT (C) measured using heat-treated and active liver S9 fraction. Active incubations were conducted in the presence and absence of NADPH and phase II cofactors. Error bars represent the standard deviation of the mean (n=3). The different lowercase letters denote significant differences between the incubation mixtures (analysis of variance and Tukey's honestly significant difference; $p < 0.05$).
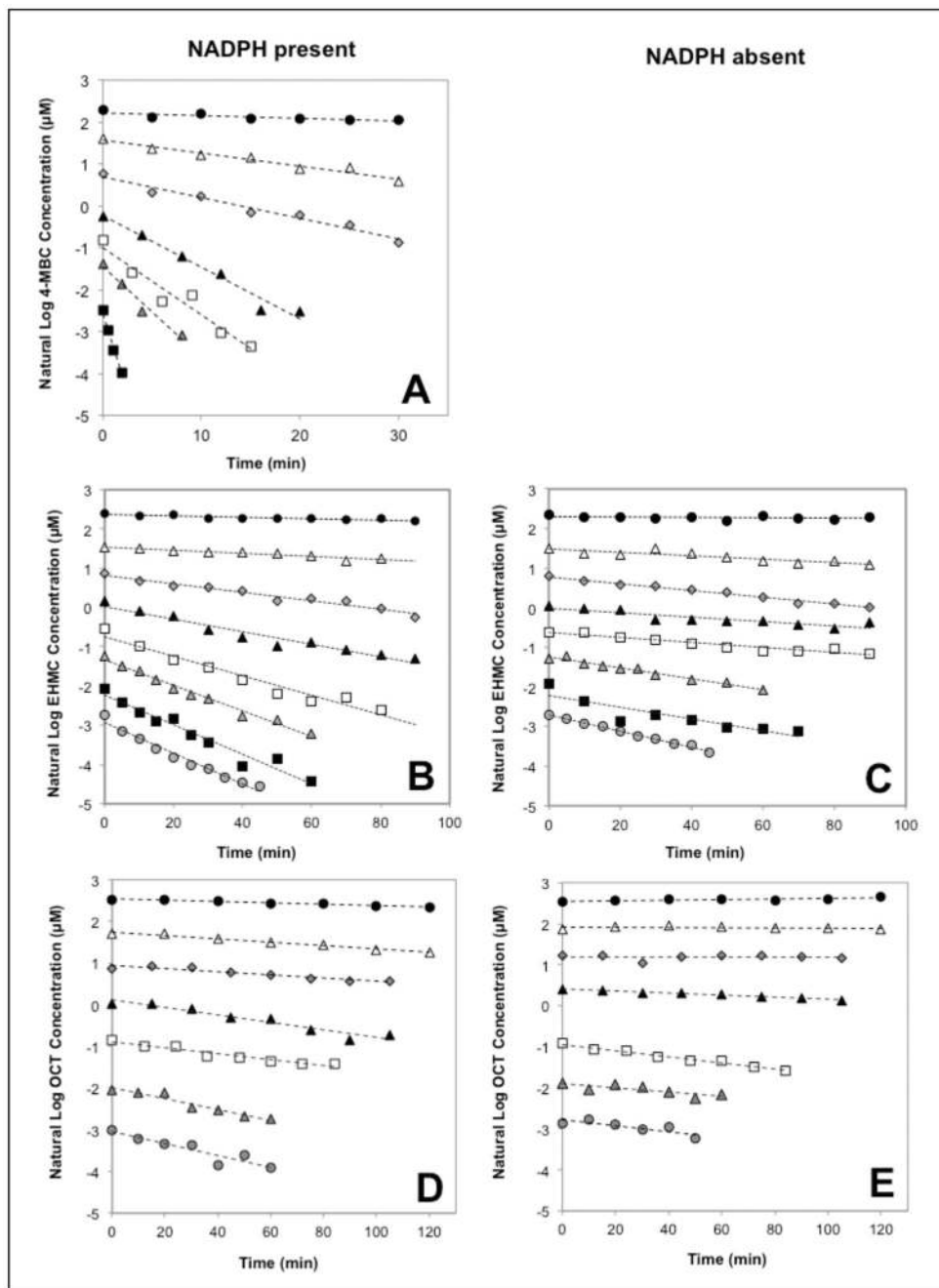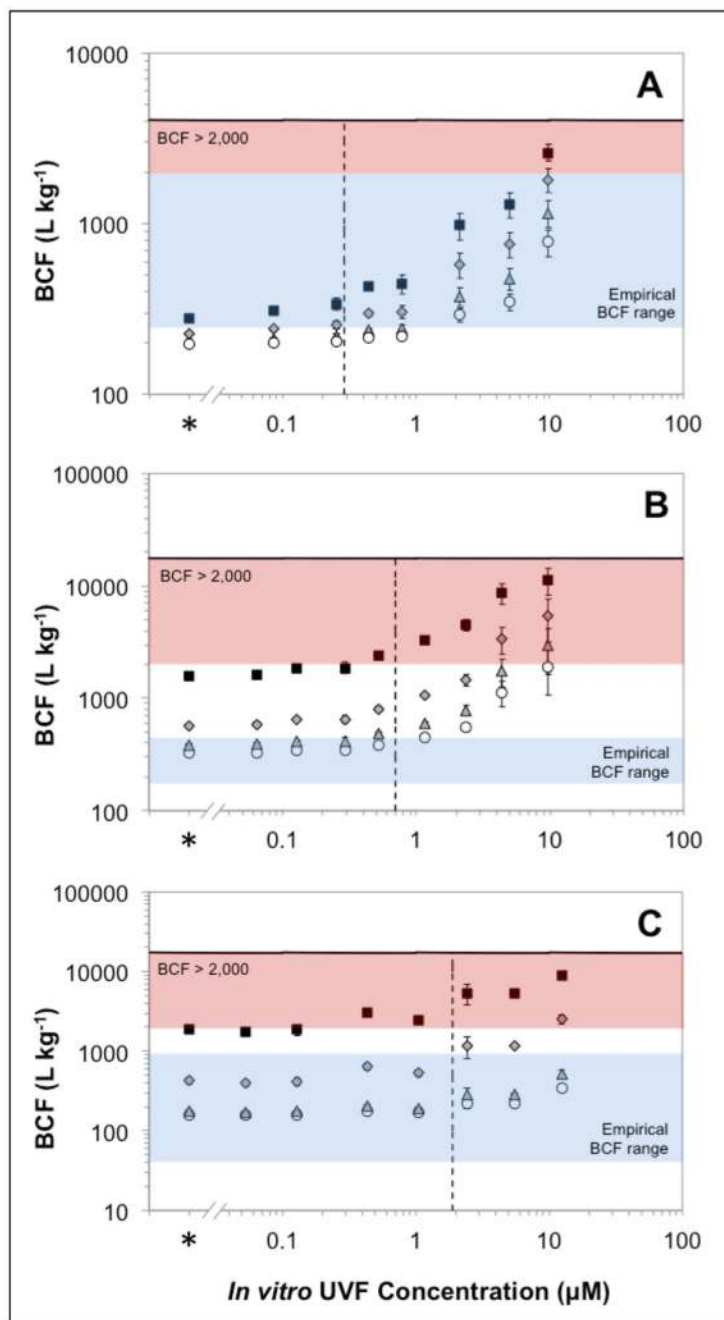
Figure 3.
Decline of the natural logarithm of the concentration of 4-MBC with added NADPH (A), EHMC with (B) and without (C) added NADPH, and OCT with (D) and without (E) added NADPH in S9 incubation medium over time (min) at various initial concentrations ranging from 0.05 to 12.5 μM.

Figure 4.
Effect of initial concentration on *in vitro* biotransformation of 4-MBC (A), EHMC (B), and OCT (C). The data presented are from incubations performed with (closed circles) and without (grey triangles) added NADPH. Error bars represent the standard deviation of the mean (n=3). Each curve was obtained by fitting Eqn. 2 to measured data using a weighted nonlinear least squares regression. Dashed lines denote the Michaelis-Menten affinity constant K_m (corresponding to the Y-axis intercept), determined from the inflection point of each fitted curve.

Figure 5.
Chemical binding in trout liver S9 fraction as a function of log K_{OW}. Measured binding values, which are plotted as the log of the bound/free ratio (log $(1-\phi_{S9}/\phi_{S9})$), are from Nichols et al. 2017 (grey circles), Nichols et al. 2013 (solid circles), Escher et al. 2011 (solid squares), Lo et al. 2015 (open triangles), and Lee et al. 2014 (grey diamonds). The lines represent binding algorithms given by Nichols et al. 2017 (dotted line), Lee et al. 2017 (dashed line), and Han et al. 2009 (solid line). All binding data were normalized to an S9 protein concentration of 2 mg mL^{-1}.

Figure 6.

Effect of *in vitro* concentration and estimated chemical binding ($f_U = \phi_P/\phi_{S9}$) on modeled bioconcentration factors (BCF) of 4-MBC (A), EHMC (B), and OCT (C). Error bars represent the standard deviation of BCFs (n=3) calculated by extrapolating each measured k_{dep} value to a whole-body biotransformation rate constant (k_{MET}; see text for details). The asterisks represent BCFs calculated using the *in vitro* depletion rate constant at an infinitesimally low substrate concentration ($k_{dep,C \to 0}$). The different BCFs calculated at each

initial concentration reflect the use of different binding models to estimate ϕ_{S9}. The models

evaluated were those given by Han et al. 2009 (solid squares), Lee et al. 2017 (grey diamonds), Nichols et al. 2017 (open circles). Additional BCFs were generated assuming that f_U= 1.0 (grey triangles). The horizontal solid lines show modeled BCFs, assuming no biotransformation (k_{dep}= 0 min^{-1}), while dashed vertical lines show the K_m value for each reaction. The red shaded areas represent BCFs that exceed regulatory bioaccumulation criteria (BCF > 2,000) and the blue shaded areas show the range of empirical BCFs for each UVF.

Table 1.

Bioaccumulation (B) metrics reported for 4-MBC, EHMC, and OCT

B Metric	4-MBC	EHMC	OCT	B Criteria	Regulatory Program
log K_{OW}	4.95	5.80	6.88	≥5.0	CEPA
BCF	251–1995[a]	175 – 433[b,c]	41– 915[d,e]	≥2000 'Bioaccumulative' ≥5000 'Very Bioaccumulative'	REACH
BAF	5,200[f]	250 – 970[g]	N/A	≥5000	CEPA
BMF	N/A	0.6 – 1.5[g]	N/A	≥1.0	NL
BSAF	N/A	0.04 – 0.3[h]	0.04 – 0.3[h]	≥1.0	NL

[a]Li et al. 2016;

[b]Nagtegaal et al. 1997;

[c]US National Library of Medicine. 2006;

[d]Blüthgen et al. 2014;

[e]Sigma-Aldrich. 2014;

[f]Nagtegaal et al. 1997;

[g]Fent et al. 2010;

[h]Gago-Ferrero et al. 2015

Log K_{OW} - Logarithmic octanol water partition coefficient; BCF - Bioconcentration Factor (L kg^{-1}); BAF- Bioaccumulation Factor (L kg^{-1});

BMF - Biomagnification Factor (kg lipid kg $lipid^{-1}$); BSAF - Biota-Sediment Accumulation Factor (kg-organic carbon kg $lipid^{-1}$); CEPA - Canadian Environmental Protection Act; REACH - Registration, Evaluation and Authorization of Chemicals; N/A – not available; NL - indicates that the B endpoint is not listed under a regulatory program

Table 2.

Kinetic parameters for *in vitro* biotransformation of UVFs by trout liver S9 fractions[a]

Kinetic parameter	4-MBC	EHMC		OCT	
	NADPH present	*NADPH present*	*NADPH absent*	*NADPH present*	*NADPH absent*
$k_{\text{dep,C}\rightarrow 0}$ (min^{-1})	0.47 (0.06)	0.042 (0.002)	0.017 (0.003)	0.015 (0.002)	0.008 (0.001)
$CL_{\text{in vitro, int}}$ (mL · h^{-1} · mg protein^{-1})	6.54 (0.79)	0.59 (0.03)	0.24 (0.04)	0.90 (0.12)	0.48 (0.06)
K_m (μM)	0.29 (0.07)	0.70 (0.07)	1.09 (0.55)	1.89 (0.57)	0.63 (0.25)
K_m (μmol · g lipid^{-1})	0.28 (0.07)	0.69 (0.10)	1.07 (0.54)	7.41 (2.24)	2.47 (0.98)
V_{max} (pmol · min^{-1} · mg protein^{-1})	31.85 (0.94)	6.84 (0.03)	4.31 (0.38)	28.35 (1.13)	5.04 (0.25)

[a] All values are reported as the mean (SE), n=3.

$k_{\text{dep,C}\rightarrow 0}$ - *in vitro* depletion rate constant at an infinitesimally low substrate concentration; $CL_{\text{in vitro, int}}$ - *in vitro* intrinsic clearance rate; K_m

- Michaelis-Menten affinity constant; V_{max} - maximum reaction velocity

Table 3.

Estimates of the fraction unbound of 4-MBC, EHMC, and OCT in trout S9 incubation media (ϕ_{S9}) and in trout plasma (ϕ_P). Calculated hepatic clearance binding correction factors ($f_U = \phi_P / \phi_{S9}$) are also provided

	4-MBC	EHMC	OCT
Fraction unbound in S9 (ϕ_{S9})			
Han et al. 2009	0.011859	0.003076	0.002411
Lee et al. 2017	0.004997	0.000709	0.000366
Nichols et al. 2017	0.002355	0.000175	0.000028
Fraction unbound in plasma (ϕ_P)			
Fitzsimmons et al. 2001	0.001277	0.000306	0.000050
Hepatic clearance binding correction factor (f_U)			
Han et al.	0.11	0.10	0.02
Lee et al.	0.25	0.43	0.14
Nichols et al.	0.54	1.75	1.77
f_U=1.0	1.00	1.00	1.00